ISSN 0016-7029, Geochemistry International, 2007, Vol. 45, No. 7, pp. 625–637. © Pleiades Publishing, Ltd., 2007.
Original Russian Text © Yu.I. Galushkin, G.E. Yakovlev, 2007, published in Geokhimiya, 2007, No. 7, pp. 691–703.

# Influence of Saline Deposits on the Conditions of Petroleum Generation in the Rocks Underlying the Salt Complex of the Northern Part of the Precaspian Basin

**Yu. I. Galushkin and G. E. Yakovlev**

*Moscow State University, Vorob'evy gory, Moscow, 119992 Russia*

*e-mail: gal@mes.msu.ru*

Received November 20, 2006

**Abstract**—Numerous studies on the potential of hydrocarbon generation by the rocks of the sedimentary cover of the northern Precaspian Basin are based either on the interpolation of measurements from a relatively sparse boreholes network or on the numerical estimations of the history of development of the hydrocarbon potential under the assumption of a steady temperature gradient both with depth in the sedimentary cover and with time during basin evolution. By the example of sedimentary sections from the northeastern part of the Precaspian Basin, variations in thermal history and petroleum formation conditions were numerically analyzed for the rocks underlying the salt complex of the basin. Variations in the temperature gradient and thermal properties of the rocks with depth and time were accounted for in the modeling. Numerical reconstructions of the thermal and maturation history of sedimentary sections from the basin were used to estimate the influence of evaporite sequences on the thermal history, the maturation level of organic matter, and the hydrocarbon generation potential of the subsalt complex of the basin. The calculations showed that this influence could be significant, but there remained an uncertainty related to the absence of reliable data on the time and rate of salt diapir formation.

**DOI:** 10.1134/S0016702907070014

## INTRODUCTION

The northern Precaspian Basin is currently an area of the extensive exploration and development of hydrocarbon deposits. However, there are very few estimates of the generation potential of the sedimentary cover of the basin. They rely either on the interpolation of measurements from a rather sparse borehole network or on the numerical estimates of the development of the hydrocarbon potential of the basin obtained assuming depth- and time-invariant temperature gradients in the history of basin subsidence. In this paper, we attempted to overcome this limitation by means of the numerical analysis of thermal history and petroleum formation conditions for the rocks underlying the salt complex of the basin, accounting for variations in the temperature gradient and thermal properties of the rocks with depth and time.

## GEOLOGICAL AND GEOPHYSICAL CHARACTERISTICS

The analysis of sedimentary sections is given in this paper by the example of the northeastern part of the Precaspian Basin along two transects extending north–south and northwest–southeast (Fig. 1). The sections are significantly different in the thickness of saline sequences (Kungurian deposits in Fig. 2), which allowed us to assess the influence of evaporite sequences on the thermal history, maturation level of organic matter (OM), and development of HC generation potential by the rocks underlying the salt complex of the basin.

The northern Precaspian petroleum basin (PB) is situated south of the Volga–Ural basin and is one of the world's deepest modern sedimentary basins. Its deep structure is largely defined by the relations in the section of three thick sedimentary units: subsalt, salt, and suprasalt sequences. The subsalt sequence includes sediments ranging in age from the Late Proterozoic to the Early Permian. It is dominated by terrigenous rocks in the eastern and southern parts of the depression and carbonate rocks in the northern and western parts. The thickness of the subsalt unit of the section ranges from 3–4 km in the marginal parts of the basin to more than 10 km in the central part [1]. The salt-bearing sequence is mainly composed of Kungurian-age salts, which occur as beds and domes. The salt domal uplifts vary in shape and size and occupy about 25–30% of the whole area of the Precaspian Basin. The thickness of salt deposits in domes may be up to 8000–9000 m and decreases up to a complete pinching out between domes. Salt is sometimes completely squeezed out in such zones, and the rocks of the suprasalt complex may rest directly on the Paleozoic rocks of the subsalt complex. Such areas are considered as promising for prospecting for oil and gas [2].

The sedimentary sequence above the salt complex of the basin is made up of terrigenous and minor car-

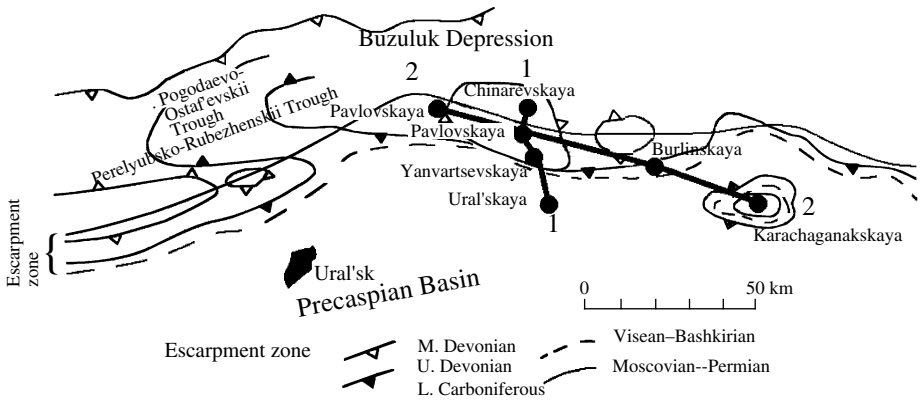


**Fig. 1.** Location of transects 1 (Chinarevskaya, Rozhkovskaya, Yanvartsevskaya, and Ural'skaya prospects) and 2 (Karachaganakskaya, Burlinskaya, and Pavlovskaya prospects) in the northern slope of the Precaspian Basin. Also shown are the positions of the escarpment bounding the basin in various periods of its development.

bonate rocks of the Late Permian, Mesozoic, and Cenozoic. Its thickness ranges from a few hundred to 1500 m at the crests of salt domes (Rozhkovskaya, Pavlovskaya, and other prospects; Fig. 2) and reaches several thousand meters in the zones between domes (Yanvartsevskaya, Burlinskaya, and other prospects; Fig. 2). The fluid isolation properties of saline deposits are well known. They are responsible for the wide occurrence of anomalous porous over pressures (APOP) in the subsalt deposits of the modern sedimentary cover of the Precaspian Basin at depths of more than 3700 m. The appearance of such pressures is most likely related to the recent neotectonic activation of the region, because, even under the most unfavorable conditions of fluid migration, the relaxation time of anomalous pressures to normal hydrostatic values is usually no higher than a few million years [3, 4].

A characteristic feature is the significant thickening of the consolidated crust of the basin from 10–15 km in the center of the Precaspian Basin (thinned crust of the rift type) to 30–40 km at its margins. Correspondingly, the Moho surface rises beneath the central part of the Precaspian Basin to depths of 32–34 km at a thickness of the overlying sedimentary deposits of up to 10–22 km (e.g., [5, 6]), whereas the crust thickens up to 40 km toward the Volga–Ural and Voronezh massifs, and the sedimentary cover reduces to 3–10 km. Up to now, there is no consensus on the mechanism of the thinning of the consolidated crust in the Precaspian Basin. It is supposed that Devonian rifting could be accompanied by crust erosion from below at the expense of eclogitization [5] or lithosphere stretching up to the oceanization of the crust [6]. In our calculations, we assumed that the basin developed (Fig. 1) on a standard continental basement, whose structure is consistent with the results of geophysical investigations and whose thermal properties are given in Table 1.

## THERMAL FIELD AND THERMAL PROPERTIES OF THE ROCKS OF THE REGION

The numerical reconstructions presented in the following sections describe the evolution of thermal regime in the sedimentary sequences of the basin on the basis of the investigation of the thermal properties of rocks and the modern thermal field of the region. The thermal field of the Precaspian Basin was most comprehensively characterized by Kotrovskii [3]. According to these data, the depth and temperature of the roof of the subsalt complex show significant local variations in the northern part of the Precaspian Basin, but, in general, the sedimentary complex is currently characterized by low and moderate temperatures in this part of the depression.

The measurements of the thermal properties of rocks from the northern Precaspian Basin gave a wide scatter, indicating significant dependence on the lithological composition of rocks, their age, and depth of occurrence [3, 9]. This fact is accounted for in the systems of basin modeling and was implemented in our reconstructions of the thermal history of the basin [10, 11]. The heat conductivities of rocks were calculated in our models using the global average values of the thermal properties of main lithological units [11, 12] and are in general agreement with the values measured in the rocks of the Precaspian Basin [3, 9, etc.]. Unfortunately, the utility of such measurements was often impaired by uncertainties in the lithological composition of rocks and the lack of data on their porosity and moisture content.

According to geothermal investigations [3, 13], the present-day heat flow in the northern part of the Caspian Basin approaches 40 mW/m$^2$. Considerable perturbations in the distribution of temperature in the sedimentary cover of this region could be caused by the formation and emplacement of salt bodies into the sedimentary sequence [2]. Salts and anhydrites show high

heat conductivities ($K$ = 3.9–5.9 W/m K), which provides a significant difference in temperature gradient between salt-bearing and salt-free sequences. For instance, the temperature at a depth of 2.5 km is about 88°C (for a temperature of $T_o$ = 20°C at the basin surface) in a shale sequence and only 38°C in saline deposits. Salt masses disturb the temperature gradient of the country rocks, such that the rocks of the upper levels of an isolated salt body may be somewhat hotter than the country rocks at the same depths far from the body, whereas the lower parts of the salt body will be always colder than the country rocks at the same depth level ([2] and see below). The temperatures of rocks from the salt body will be similar to those of the country rocks only at intermediate depth levels. Although the timing and mechanisms of salt diapir formation remain controversial, there is no doubt that these structures experienced considerable changes during the geologic history of the basin, which resulted in disturbances in the depth distribution of rock temperature during the formation of salt structures.

## EVOLUTION OF THE THERMAL REGIME OF THE NORTHERN SLOPE OF THE PRECASPIAN BASIN: NUMERICAL RECONSTRUCTION

The burial and thermal evolution of the sedimentary sequence of the northern slope of the Precaspian Basin was characterized in this paper by the example of seven sedimentary sections at the Ural'skaya, Karachaganakskaya, Chinarevskaya, Pavlovskaya, Burlinskaya, Yanvartsevskaya, and Rozhkovskaya prospects located along two transects oriented north–south and northwest–southeast (Fig. 1). Reconstructions were carried out using the GALO program package for basin modeling [10–12, 14], which allows numerical estimation of the evolution of the thermal regime, catagenesis, and degree of source potential realization of sedimentary basins. The results of numerical modeling for the thermal and maturation history of the basin are shown in Fig. 2. Variations in the burial depth of the sedimentary layers of the basin are shown in these diagrams by solid lines. The corresponding reconstructions were carried out using the well-known procedure of backstripping assuming that the porosity of rocks in every lithologically homogenous layer decreases with depth following an exponential law, whose parameters depend on the lithology of the given layer [10–12, 14]. The modern section of the sedimentary sequence of the basin is exemplified in Table 2 by the section of the Chinarevskaya prospect, and Fig. 2 shows the petrographic characteristics of sediments, which are needed for the estimation of the parameters of rock compaction with depth and formed the initial database for the reconstruction of burial history.

The evolution of thermal regime in the sedimentary sequence of the northern slope of the northern Precaspian Basin is illustrated in Fig. 2 by the distribution of isotherms. The thermal history of the sections was reconstructed by modeling heat transfer in the sedimentary sequence, crust, and mantle on the basis of the solution of a nonsteady-state one-dimensional equation for heat transfer with allowance for the compaction of sedimentary rocks depending on their lithology and burial depth. Temperatures were calculated accounting for variations in the thermal properties of rocks related to changes in porosity, lithology, temperature, and pressure during the whole history of basin subsidence [10–12, 14]. The temperature distribution was calculated for the sedimentary layer and the basement; the properties of rocks are given in Table 1. A temperature of about 1160°C was kept at the base of the calculation domain at a depth of 130–170 km. Figure 3 shows the evolution of temperature in the lithosphere of the basin obtained by the numerical modeling of the Chinarevskaya prospect. In general, our modeling implies that the lithosphere of the northern Precaspian Basin underwent cooling from the initial epirift state of the lithosphere with a surface heat flow of 60-100 mW/m$^2$ in the Middle Devonian to a moderate present-day heat flow of 40–45 mW/m$^2$ (Fig. 3). The latter values are in agreement with the measurements of heat flow in the region (e.g., [3, 13]).

**Table 1.** Structure of the continental lithosphere and rock properties [7]

| Parameter | Layer | | | |
|---|---|---|---|---|
| | Granitic | | Basaltic | Mantle |
| Depth of layer bottom, km | 5.0 | 15.0 | 35.0 | >35 |
| Density, g/cm$^3$ | 2.75 | 2.75 | 2.90 | 3.30 |
| Heat conductivity, W/m K | 2.72 | 2.72 | 1.88 | K = $f$ ($T$)* |
| Heat generation, μW/m$^3$ | 1.26 | 0.71 | 0.21 | 0.004 |

* According to Schatz and Simmons [8], $f(T) = K_0$ {88.33/[31. + 0.21($T$°C + 273.15)]} at $T \le 226.85$°C and $f(T) = K_0$ {88.33/[31. + 0.21($T$°C + 273.15) + 4.86 × 10$^{-4}$($T$°C –226.85°C)]} at $T > 226.85$°C, where $K_0$ = 4.731 W/m K, and $T$ is temperature in °C.

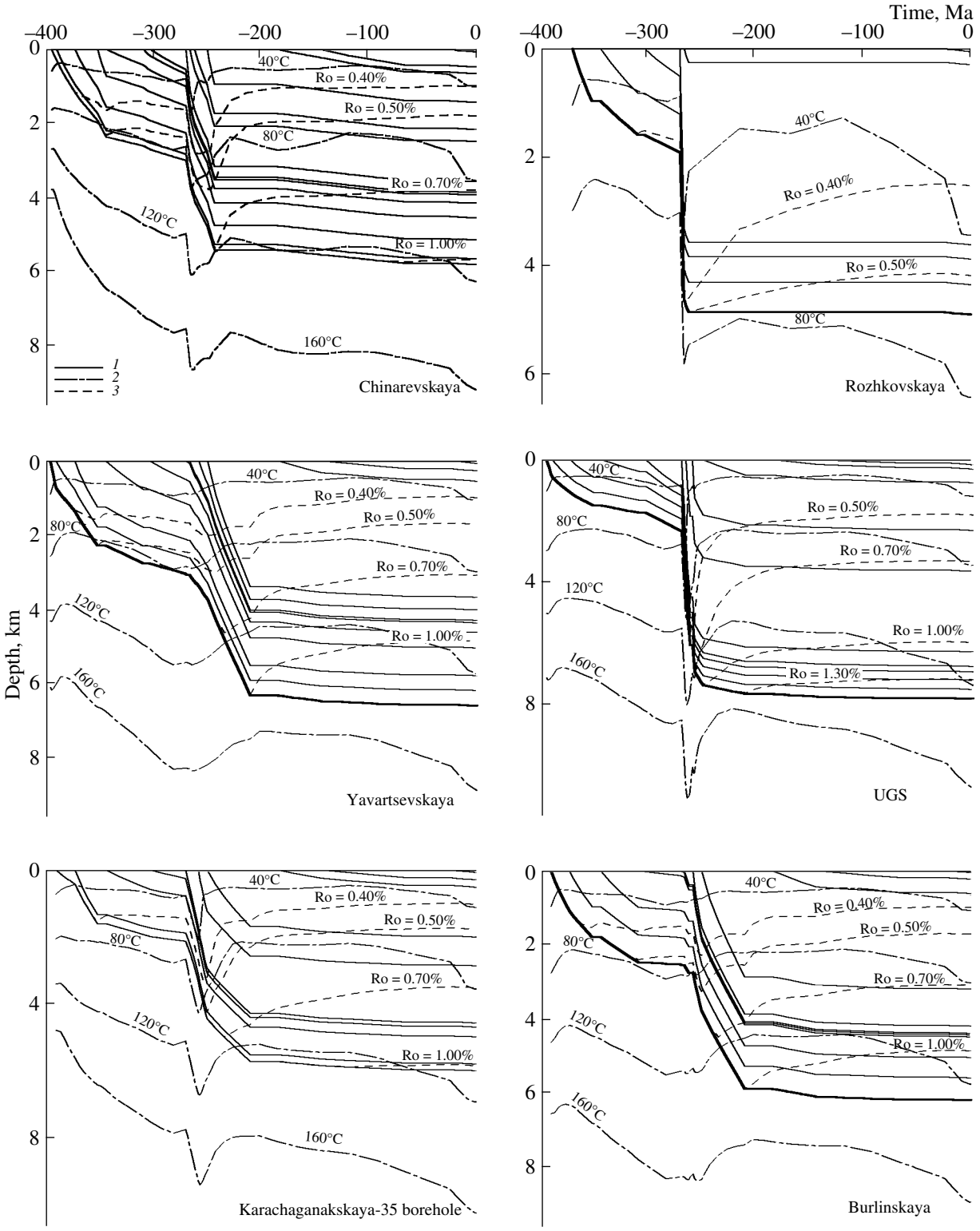


**Fig. 2.** Numerical reconstructions of subsidence history, thermal regime, and organic matter maturity for the sedimentary sequences from four prospects of transect 1 (Chinarevskaya, Rozhkovskaya, Yanvartsevskaya, and Ural'skaya) and three prospects of transect 2 (Karachaganakskaya, Burlinskaya, and Pavlovskaya) in the northern slope of the Precaspian Basin. The lower right panel shows variations in the surface temperature of the basin (paleoclimate) [15, 16] that were used in our modeling. The location of transects and prospects is shown in Fig. 1. (*1*) Bottom depth of a sedimentary layer, (*2*) isotherm, and (*3*) vitrinite reflectance (%Ro).

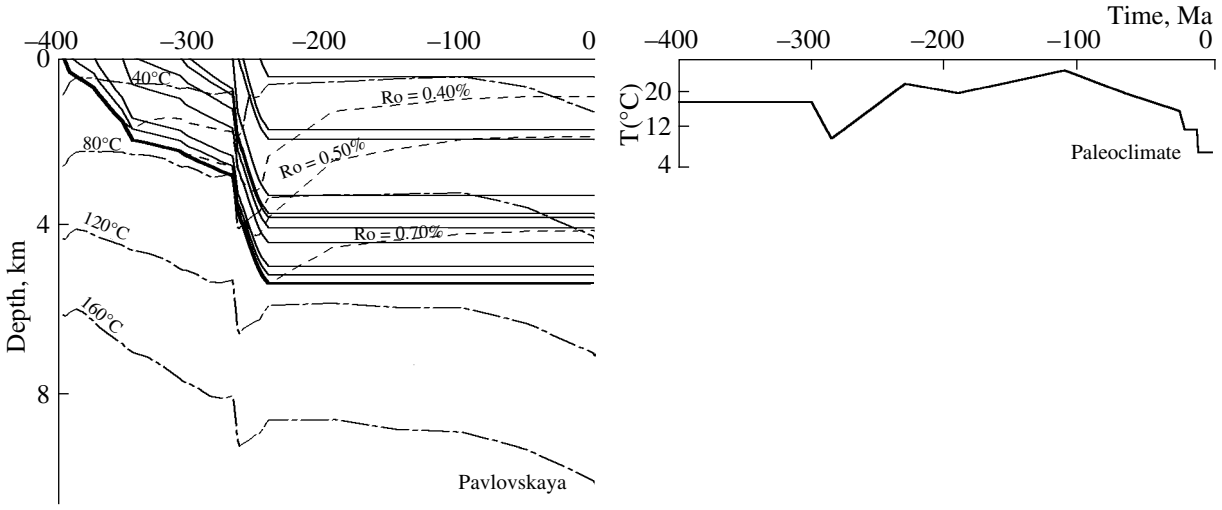


**Fig. 2.** Continued.

Our modeling relied heavily on the analysis of the tectonic subsidence of the basin. It was assumed that the supposed sequence of thermal and tectonic events in the lithosphere of the basin should be consistent with variations in the amplitude of tectonic subsidence of the basement surface. Then, for those periods of basin development when the response of its lithosphere to loading was isostatic, variations in the tectonic subsidence of its basement calculated after the removal of water and sediment loading from the basement surface (upper solid line in the left panel of Fig. 4) must be similar to variations in tectonic amplitudes calculated from the depth distribution of rock density in the basement [10–12, 14]. The latter variations were calculated taking into account density changes due to the supposed thermal and tectonic (extension) events in the history of the basin (upper dashed curve in Fig. 4a). The agreement between the two tectonic curves was reached for the areas of the northern slope of the Precaspian Basin considered here assuming that the moderate thermal activation of the lithosphere with an effective surface heat flow of 50–55 mW/m$^2$ occurred from the Late Devonian to the Kungurian, whereas Late Permian time was marked by minor lithosphere stretching with an amplitude of about 1.05 (Figs. 3, 4).

The agreement of the calculated values of temperatures and vitrinite reflectance with measurements in the modern sedimentary section is considered as an important criterion for the consistency of the accepted model of the thermal development of the basin. However, direct temperature measurements were available only for two prospects, Karachaganakskaya and Chinarevskaya (these data are shown for the latter prospect in Fig. 4b). Furthermore, the temperature values reported in [3] for depths of 500, 1000, 2000, and 3000 m and the roof of the subsalt complex were obtained by the interpolation of data for a very sparse borehole network and can be used only for very rough temperature estimates in particular areas of the basin. In general, both the measured and estimated temperatures were in agreement with the model values. The calculations showed that the temperature regime of rocks is strongly dependent on the rate and amplitude of basin subsidence, the lithology of rocks composing its sedimentary section and, especially, the thickness and burial depth of saline deposits in the section. In particular, the calculations showed that temperature values of about 100°C are reached at depths of 4.0–4.5 km in the sequences with the thinnest salt beds (less than 100 m in the Yanvartsevskaya and Burlinskaya prospects) and at much greater depths (5.5–6.0 km) in the sedimentary sequences of the Ural'skaya, Karachaganakskaya, and Pavlovskaya prospects, which host thick salt beds (Fig. 2). In the present-day distribution of temperature with depth, the influence of salt is manifested in the existence of areas with significantly lower temperature gradients (Figs. 2, 4). The cooling effect of salt is most distinctly illustrated by the thermal regime of the Rozhkovskaya prospect, where thick salt beds occur near the surface and, as a result, the temperature of rocks is no higher than 60°C even at depths of about 5 km (Fig. 2).

Lateral heat transfer can strongly reduce horizontal temperature variations in a two-dimensional ($x$, $z$) thermal section of a basin constructed by the linear approximation of a series of one-dimensional (along $z$) reconstructions. Figure 5 allows us to estimate the expected temperature deviations from the values obtained by numerical reconstructions in a planar basin approximation (Figs. 2, 4). As could be expected, temperatures calculated with allowance for lateral heat transfer will be higher than the one-dimensional values within salt diapirs and in the underlying sequences and somewhat lower outside the diapirs (Fig. 5). The correction is no higher than 5°C for all depth levels within sedimentary complexes occurring between the diapirs and far from them at distances of 5–10 km. In accordance with these

**Table 2.** Main evolution stages of the northern slope of the Precaspian Basin in the region of the Chinarevskaya prospect

| *N* | Evolution stage | Geologic time, Ma | Depth, m | Lithology; cl : si : sa : li : do : sl : an | Paleoclimate, °C |
|---|---|---|---|---|---|
| 1 | Sedimentation | 0–24 | 0–64 | 50 : 00 : 50 : 00 : 00 : 00 : 00 | 7–16 |
| 2 | Hiatus | 24–65 | 64 | – | 16–20 |
| 3 | Sedimentation | 65–144 | 64–471 | 50 : 00 : 00 : 50 : 00 : 00 : 00 | 20–25 |
| 4 | Sedimentation | 144–184 | 471–648 | 40 : 00 : 40 : 20 : 00 : 00 : 00 | 20–22 |
| 5 | Hiatus | 184–243 | 648 | – | 20–22 |
| 6 | Sedimentation | 243–250 | 648–1411 | 50 : 00 : 50 : 00 : 00 : 00 : 00 | 19 |
| 7 | Sedimentation | 250–262 | 1411–2150 | 20 : 20 : 20 : 00 : 00 : 30 : 10 | 18 |
| 8 | Sedimentation | 262–266 | 2150–2480 | 30 : 40 : 30 : 00 : 00 : 00 : 00 | 17 |
| 9 | Sedimentation | 266–270 | 2480–3570 | 00 : 00 : 00 : 00 : 00 : 100 : 00 | 15 |
| 10 | Sedimentation | 270–303 | 3570–3860 | 00 : 00 : 00 : 80 : 20 : 00 : 00 | 10–15 |
| 11 | Sedimentation | 303–309 | 3860–3930 | 80 : 00 : 20 : 00 : 00 : 00 : 00 | 15–17 |
| 12 | Sedimentation | 309–344 | 3930–4150 | 00 : 00 : 00 : 70 : 30 : 00 : 00 | 17–18 |
| 13 | Sedimentation | 344–352 | 4150–4540 | 10 : 00 : 00 : 45 : 45 : 00 : 00 | 18 |
| 14 | Sedimentation | 352–373 | 4540–5140 | 00 : 00 : 00 : 70 : 30 : 00 : 00 | 18 |
| 15 | Sedimentation | 373–390 | 5140–5650 | 30 : 00 : 00 : 30 : 40 : 00 : 00 | 18 |
| 16 | Sedimentation | 390–395 | 5650–5800 | 30 : 00 : 70 : 00 : 00 : 00 : 00 | 18 |

Note: Depth values indicate the present-day position of the lower and upper boundaries of the sedimentary layer. The column "Lithology" gives percentages of main lithological units in the rocks of the layer in the sequence: cl, clay; si, siltstone; sa, sandstone; li, limestone; do, dolomite; sl, salt; and an, anhydrite.

considerations, temperatures in the salt and subsalt complexes of the Rozhkovskaya borehole should be 10–15°C higher compared with the results presented in Fig. 2. In contrast, the temperatures of the suprasalt and subsalt complexes of the Chinarevskaya, Yanvartsevskaya, and Ural'skaya boreholes, which are located far from salt diapirs, could be 3–10°C lower than those calculated in one-dimensional reconstructions (Figs. 2, 4).

## EVOLUTION OF MATURATION CONDITIONS OF ORGANIC MATTER IN THE SEDIMENTS OF THE NORTHERN SLOPE OF THE PRECASPIAN BASIN: NUMERICAL ESTIMATES

Based on the calculated temperatures during rock burial, the degree of organic matter (OM) maturation in the rocks was numerically estimated by calculating the vitrinite reflectance (%Ro) using the kinetic spectrum of vitrinite maturation from [17, 18]. Figure 2 shows %Ro isolines, and Fig. 4c exemplifies the calculated distribution of %Ro with depth in the modern sedimentary sequence of the Chinarevskaya prospect. Table 3 gives the degrees of OM maturation in the rocks of the base of supposed source sequences of the basin areas studied. According to our estimates, the major zone of oil formation (MZOF) (Ro > 0.70%) includes the deposits of the modern suprasalt complex at depths of 3–4 km at the Ural'skaya, Yanvartsevskaya, and Burlinskaya prospects and the rocks of the subsalt complex at depths of 4.0–4.5 km in the Karachaganakskaya, Chinarevskaya, and Pavlovskaya prospects (Fig. 2, 4c). Within the low-temperature Rozhkovskaya prospect, the degree of maturation is estimated as no higher than Ro = 0.60% at the base of the subsalt complex (Fig. 2, Table 3). Thus, the rocks of the suprasalt and subsalt complexes of the northern slope of the Precaspian Basin show diverse OM maturation conditions.

There are a number of estimates in the literature for the degree of OM maturation in the sedimentary sequence of the Precaspian Basin, which can be compared with the results of our modeling. For instance, Zaurbekov [9] estimated the degree of OM maturation in rocks (expressed as %Ro) for various depth intervals in the eastern part of the Precaspian Basin. Although these data are in general consistent with the calculations shown in Figs. 2 and 4, their utility is strongly lowered by the lack of information on the position of samples in the stratigraphic section and boreholes. Konyukhova [19] estimated the degree of OM maturation in the Devonian and Carboniferous rocks underlying the salt complex on the basis of the element analysis (H/C–O/C) of kerogen using the Van Krevelen–Hunt diagram and sterane and trepan maturity parameters. According to her analysis, the main zone of oil generation was reached by the Devonian, Carboniferous, and even Permian rocks, provided the basin subsided to depths of no less than 3.5–4.0 km, which is in agreement with our calculations (Table 3). However, the degrees of OM maturity reported by Konyukhova [19] for the Karachaganaksaya and Chinarevskaya prospects seem to be underestimated. For instance, her anal-

ysis suggested that the maturation conditions of OM from the Middle Devonian–Frasnian deposits of the Chinarevskaya and Karachaganakskaya prospects correspond to the early stage of the oil window, at a transition from $MK_1$ to the beginning of $MK_2$ ($0.5 < Ro < 0.7\%$), whereas our estimates indicate the mature part of the window ($0.8 < Ro < 1.02\%$). It can also be pointed out that the conclusions of Konyukhova are in conflict with, first, the great depths of occurrence of these formations at the areas considered (5000–6000 m, Table 3); second, the low values of hydrogen index (HI) in these rocks (8–170 mg HC/g $C_{org}$ in the Karachaganskaya prospect and 30–75 mg HC/g $C_{org}$ in the Chinarevskaya prospect [19]); and, third, the relatively high $T_{max}$ values [19]. There is also evidence for the inflow of light low-sulfur oil from depths of 5647–5754 m at the Karachaganakskaya prospect (at pressures of $P$ = 50–59 MPa and formation temperatures of $T$ = 95–113°C) and an oil–gas–water mixture from depths of 6120–6218 m, which is again in better agreement with our data from Table 3 than with the estimates of Konyukhova [19].

The values of vitrinite reflectance, %Ro, calculated in this study are compared in Table 4 with data from a report obtained by means of the French program package GENEX. The reported depths correspond to rocks with different degrees of OM maturity in the modern sedimentary sequence of the northern slope of the Precaspian Basin. The discrepancies between the maturity estimates presented in Table 4 are related to the different geothermal histories of rocks used in the two studies. In our paper, the GALO system (see above) was separately used to calculate the burial history of each particular area. The distribution of temperature and thermal gradient in the sedimentary sequence varied not only with depth and between areas but also with time during the basin subsidence (Figs. 2, 4). Modeling in the GENEX system involves maturity calculation assuming a constant temperature gradient both with depth and with time during basin development (Table 4), and these exercises provide, therefore, averaged characteristics. The degree of maturation is evidently overestimated at great depths in salt-free sequences and underestimated in the suprasalt complexes in sequences with relatively deep occurrence of salt beds.

Lateral heat transfer must change to some extent the results of reconstructions obtained in the model of a planar basin. It was already noted that higher temperatures (by 10–15°C) should be expected in the salt and subsalt complexes of the Rozhkovskaya borehole compared with the results shown in Table 2, and the degree of OM maturity in its subsalt complex must therefore be higher. In contrast, the temperatures of the suprasalt and subsalt complexes in the Chingarevskaya, Yanvartsevskaya, and Ural'skaya boreholes, which are located outside the salt diapirs, could be 3–10°C lower than those calculated in the one-dimensional reconstructions (Figs. 2, 4). The real degree of OM maturity in these boreholes can probably be slightly lower than that

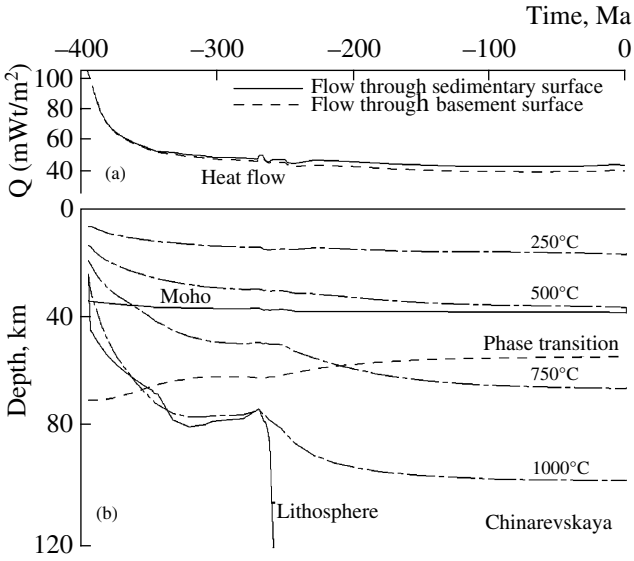


**Fig. 3.** (a) Heat flow and (b) thermal evolution of the lithosphere in the geologic history of the northern slope of the Precaspian Basin at the region of the Chinarevskaya prospect (numerical reconstruction).

shown in the figures. Unfortunately, it is difficult to estimate quantitatively the decrease in the degree of maturity due to lateral heat transfer. It is obvious that the influence of the aforementioned temperature changes on the degree of OM maturation must be significant in old salt diapirs. In contrast, it should have been negligible if the diapirs were formed recently. However, the timing of formation and growth rates of the salt diapirs are not constrained, and the problem remains unsolved.

## REALIZATION OF THE PETROLEUM POTENTIAL OF SUPPOSED SOURCE ROCK IN THE NORTHERN SLOPE OF THE PRECASPIAN BASIN

The reconstruction of the thermal history of a basin provides insight into the degree of the realization of the petroleum potential of the supposed source rocks [10, 18]. Table 5 shows the type of OM, the initial potential of HC generation, and OM content in the rocks of the region that were accepted in our modeling. It can be seen that these parameters are different for the northern and southern groups of prospects. In particular, the rocks of the southern group have a higher initial potential of HC generation than the sequences of the same age from the northern group. Variations in the burial depth, temperature, and %Ro values in the subsidence history of the main supposed source formations of the basin are shown in Table 3 and Figs. 2, 6.

Our modeling suggested a degree of OM maturation corresponding mainly to $Ro > 1\%$ for the rocks occurring in the present-day section of the basin at depths greater than 6 km (Fig. 2, Table 3). The Devonian source rocks buried to depths of greater than 5 km are

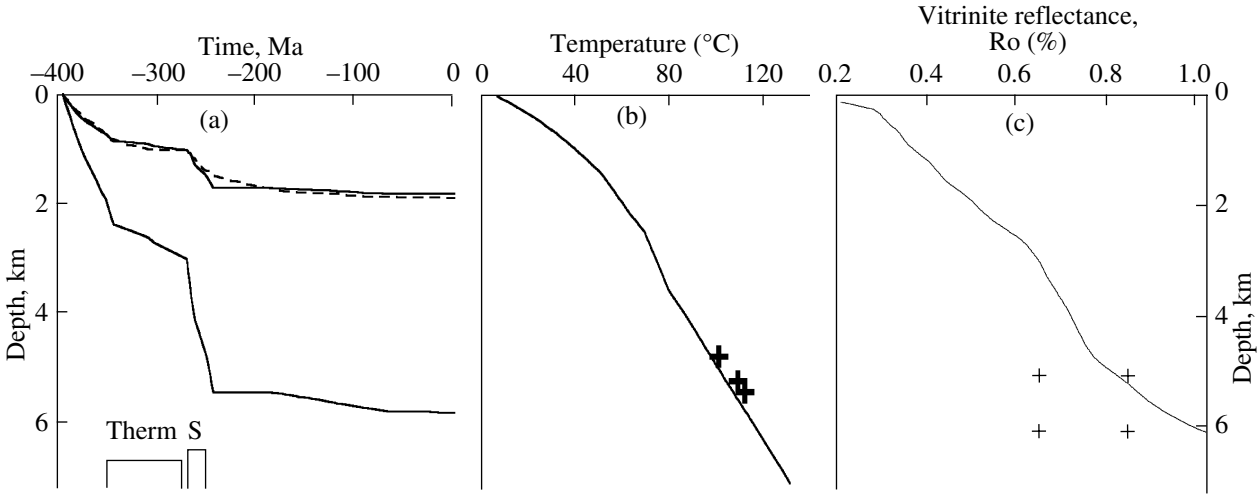


**Fig. 4.** (a) Real and tectonic subsidence of the basement top in the history of basin development, (b) present-day distribution of temperature with depth, and (c) vitrinite reflectance calculated for the sedimentary section of the northern slope of the Precaspian Basin at the region of the Chinarevskaya prospect. (a) The lower solid curve shows the real depth of basement subsidence calculated by the procedure of backstripping; the upper solid curve is the tectonic subsidence of the basement surface calculated by eliminating the loading of water and sediments; the dashed line shows the tectonic subsidence obtained from the analysis of variations in density distribution in the basement column. "Therm" denotes the thermal activation of the lithosphere in the Carboniferous and Early Permian to an effective surface heat flow of 50–55 mW/m$^2$, and "S" marks the period of the maximum lithosphere stretching in the Late Permian with an amplitude of 1.05 (see text for explanation). The solid curves in panels (b) and (c) are the calculated temperature and %Ro distributions with depth in the present-day section of the basin. The crosses denote the measured temperatures and rough estimates for the basin-average degrees of OM maturation for the given depth interval according to the published data.

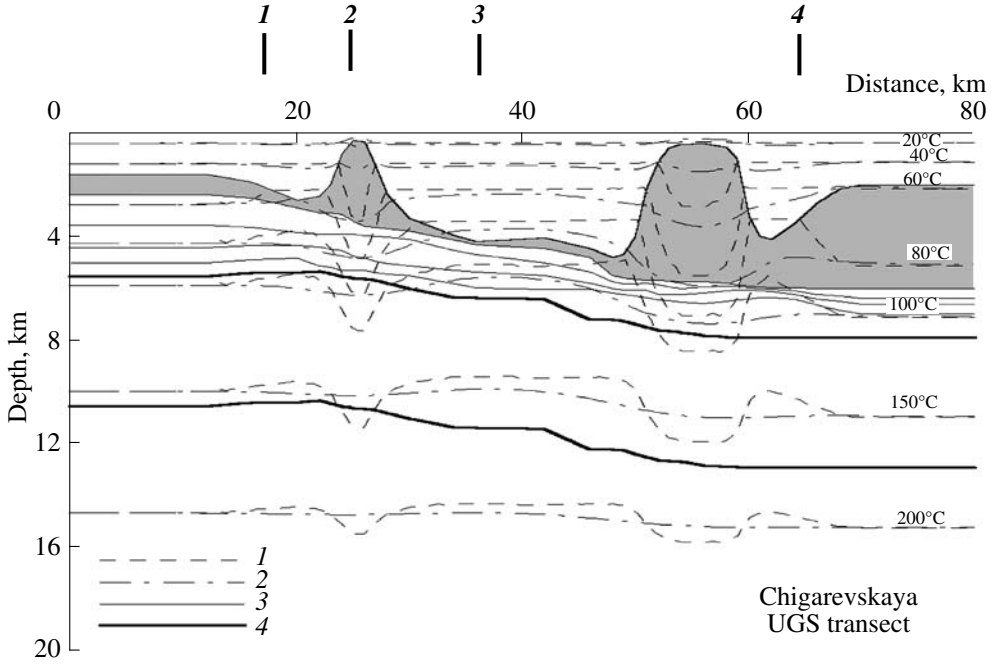


**Fig. 5.** Comparison of temperature distributions calculated by one-dimensional and two-dimensional steady-state models for the region of salt diapir occurrence in the northern part of the Precaspian Basin along a transect crossing the (*1*) Chinarevskaya, (*2*) Rozhkovskaya, (*3*) Yanvartsevskaya, and (*4*) Ural'skaya prospects. The areas of occurrence of salt layers and diapirs are shown by gray shading. (*1*) Calculations in the one-dimensional (flat) approximation, (*2*) calculations in the two-dimensional approximation, (*3*) boundaries of sedimentary layers, and (*4*) top and bottom of the upper 5-km portion of the granitic layer.

**Table 3.** Calculated degrees of OM maturity (represented by %Ro), temperatures, and realization of the potential of HC generation for the supposed source rocks beneath the salt complex of the northern slope of the Precaspian Basin

| t | *Z* | *T* | Ro | Hi | $H_t$ | $H_0$ | $H_g$ | $t_1$ | $t_{exp}$ | $t_2$ |
|---|---|---|---|---|---|---|---|---|---|---|
| Ma | m | °C | % | mg HC/g $C_{org}$ | | | | Ma | | |
| *Ural'skaya prospect* | | | | | | | | | | |
| 395 | 7800 | 124.4. | 1.442 | 312 | 299 | 150 | 109 | 263 | 254.8 | 192 |
| 373 | 7200 | 116.9 | 1.275 | 627 | 603 | 497 | 69.8 | 261 | 256 | – |
| 352+ | 6930 | 113.2 | 1.194 | 543.5 | 543 | 485 | 57.5 | 260 | 245 | – |
| 352– | 6930 | 113.2 | 1.194 | 543.5 | 543 | 485 | 57.5 | 260 | 251.7 | – |
| 309 | 6750 | 111.1 | 1.160 | 377 | 377 | 301 | 70.5 | 259.5 | 205.3 | – |
| 270+ | 6275 | 106.5 | 1.081 | 377 | 374 | 307 | 65.7 | 258.1 | – | – |
| *Karachaganakskaya prospect* | | | | | | | | | | |
| 390 | 6000 | 106.6. | 1.022 | 312 | 282 | 223 | 59 | 253.9 | 216.7 | – |
| 373 | 5800 | 104.1 | 0.967 | 627 | 523 | 502 | 21 | 249.7 | 228 | – |
| 352+ | 4990 | 94.1 | 0.833 | 543.5 | 209 | 181 | 28 | 242.6 | – | – |
| 352– | 4990 | 94.1 | 0.833 | 543.5 | 209 | 181 | 28 | 242.6 | – | – |
| 309 | 4744 | 89.8 | 0.782 | 377 | 184 | 152 | 32 | 238.8 | – | – |
| 270+ | 4575 | 88.4 | 0.771 | 377 | 163 | 134 | 29 | 237.1 | – | – |
| *Chinarevskaya prospect* | | | | | | | | | | |
| 395 | 5800 | 111.9. | 1.019 | 225.1 | 165 | 108 | 57 | 346.5 | – | – |
| 373 | 5140 | 102.4 | 0.863 | 377 | 300 | 248 | 52 | 257.1 | – | – |
| 352+ | 4540 | 94.0 | 0.776 | 377 | 172 | 142 | 30 | 246.8 | – | – |
| 352– | 4540 | 94.0 | 0.776 | 268.5 | 98.9 | 75 | 23.9 | 246.8 | – | – |
| 309 | 3930 | 84.7 | 0.711 | 268.5 | 34.6 | 25.6 | 9 | 242.3 | – | – |
| 270+ | 3570 | 79.8 | 0.666 | 268.5 | 14.8 | 10.6 | 4.2 | 238.3 | – | – |
| *Pavlovskaya prospect* | | | | | | | | | | |
| 395 | 5400 | 94.7. | 0.849 | 225.1 | 114 | 80 | 34 | 305.0 | – | – |
| 373 | 5000 | 88.8 | 0.784 | 377 | 188 | 156 | 32 | 255.0 | – | – |
| 352+ | 4440 | 81.0 | 0.725 | 377 | 75.6 | 62.3 | 13.3 | 248.4 | – | – |
| 352– | 4440 | 81.0 | 0.725 | 268.5 | 44.4 | 33.2 | 11.2 | 248.4 | – | – |
| 309 | 3845 | 72.6 | 0.659 | 268.5 | 12.8 | 9.13 | 3.67 | 242.5 | – | – |
| 270+ | 3314 | 64.2 | 0.607 | 268.5 | 2.76 | 1.91 | 0.85 | 232.4 | – | – |
| *Burlinskaya prospect* | | | | | | | | | | |
| 390 | 6200 | 124.5. | 1.305 | 225.1 | 189 | 105 | 78 | 310 | 221 | 29.7 |
| 373 | 5600 | 116.7 | 1.156 | 377 | 377 | 309 | 66 | 248.5 | 116.7 | – |
| 352+ | 5050 | 109.9 | 1.036 | 377 | 371 | 310 | 62 | 242.9 | – | – |
| 352– | 5050 | 109.9 | 1.036 | 268.5 | 226 | 168 | 58 | 242.9 | – | – |
| 309 | 4490 | 102.3 | 0.901 | 268.5 | 194 | 148 | 46 | 236 | – | – |
| 270+ | 4438 | 101.7 | 0.893 | 268.5 | 190 | 145 | 45 | 235.4 | – | – |
| *Yanvartsevskaya prospect* | | | | | | | | | | |
| 395 | 6600 | 130.5. | 1.415 | 312 | 299 | 164 | 102 | 353 | 219 | 148 |
| 373 | 5800 | 119.8 | 1.195 | 627 | 599 | 529 | 51 | 247.4 | 224.5 | – |
| 352+ | 5050 | 110.4 | 1.036 | 543.5 | 497 | 445 | 52 | 237.7 | – | – |
| 352– | 5050 | 110.4 | 1.036 | 543.5 | 497 | 445 | 52 | 237.7 | 201 | – |
| 309 | 4630 | 104.7 | 0.928 | 377 | 348 | 290 | 58 | 232.7 | – | – |
| 270+ | 4370 | 101.2 | 0.883 | 377 | 320 | 266 | 54 | 229.7 | – | – |
| Rozhkovskaya prospect | | | | | | | | | | |
| 373 | 4900 | 58.2 | 0.564 | 377 | 1.64 | 1.35 | 0.29 | 232.1 | – | – |
| 352+ | 4350 | 50.9 | 0.511 | 377 | 0.335 | 0.276 | 0.059 | 125 | – | – |
| 352– | 4350 | 50.9 | 0.511 | 268.5 | 0.234 | 0.159 | 0.075 | 125 | – | – |
| 309 | 3880 | 44.8 | 0.466 | 268.5 | 0.0535 | 0.036 | 0.0175 | 236 | – | – |
| 270+ | 3617 | 41.1 | 0.441 | 268.5 | 0.0227 | 0.0153 | 0.0074 | 235.4 | – | – |

Note: t is the age of formation, Ma. *Z* is the depth in the modern section in km. *T* is temperature in °C. Ro is the effective vitrinite reflectance in % (see text). Hi is the initial potential of HC generation by the rocks of the formation. $H_t$ is the total generation of HC by the source rocks. $H_0$ and $H_g$ are the generation of liquid and gas HC, respectively. $t_1$ and $t_2$ are the times of rock entering into the oil (Ro = 0.50%) and gas (Ro = 1.30%) windows. $t_{exp}$ is the time of attainment of the threshold of primary emigration, when liquid HC fill 20% of the pore space. The types of kerogen and the initial potentials of HC generation correspond to the data of Table 5.

**Table 4.** Comparison of depths corresponding to various degrees of OM maturation estimated for the modern section using the GENEX software program with a constant temperature gradient and the GALO system used in this study

| Prospect | Calculated depths corresponding to various degrees of OM maturation, km | | | |
|---|---|---|---|---|
| | Ro = 0.70% | Ro = 1.00% | Ro = 1.30% | Ro = 2.00% |
| *Prospects with negligible fractions of salts in sedimentary sequences* | | | | |
| d*T*/dz = 20°C/km (GENEX) | 2.900 | 3.900 | 4.300 | 5.200 |
| Burlinskaya (GALO) | 3.100 | 4.880 | 6.100 | – |
| Yanvartsevskaya (GALO) | 3.080 | 4.870 | 6.080 | – |
| *Prospects with thick salt beds in sedimentary sections* | | | | |
| d*T*/dz = 15°C/km (GENEX) | 4.400 | 5.800 | 6.600 | 7.500 |
| UGS (GALO) | 3.320 | 5.960 | 7.150 | – |
| Karachaganakskaya (GALO) | 3.510 | 5.850 | – | – |
| Chinarevskaya (GALO) | 3.810 | 5.720 | – | – |
| Pavlovskaya (GALO) | 4.140 | – | – | – |

**Table 5.** Type and content of OM and the initial potential of HC generation for the supposed source formation of the northern slope of the Precaspian Basin

| Age of formation, Ma | Supposed OM type | Initial potential of HC generation, mg HC/g $C_{org}$ | $C_{org}$ |
|---|---|---|---|
| *Burlinskaya, Chinarevskaya, Rozhkovskaya, and Pavlovskaya prospects* | | | |
| 395 (Emsian) | 30% ker II (377) + 70% ker III (160) | 225.1 | 1.2% |
| 373 (Late Frasnian) | ker II (377) | 377 | 0.5% |
| 352 (Tournaisian) | ker II (377) | 377 | 0.4% |
| 352 (Bobrikovskian) | 50% ker II (377) + 50% ker III (160) | 268.5 | 1.0% |
| 309 (Vereiskian) | 50% ker II (377) + 50% ker III (160) | 268.5 | 0.6% |
| 270 (Artinskian) | 50% ker II (377) + 50% ker III (160) | 268.5 | 0.3% |
| *Ural'skaya, Yanvartsevskaya, and Karachaganakskaya prospects* | | | |
| 395 (Emsian) | 70% ker II (377) + 30% ker III (160) | 311.9 | 0.8% |
| 373 (Late Frasnian) | ker II (627) | 627 | 1.5% |
| 352 (Tournaisian) | 50% ker I (710) + 50% ker II (377) | 543.5 | 0.4% |
| 352 (Bobrikovskian) | 50% ker I (710) + 50% ker II (377) | 543.5 | 1.0% |
| 309 (Vereiskian) | ker II (377) | 377 | 0.3% |
| 270 (Artinskian) | ker II (377) | 377 | 0.3% |

Note: ker denotes kerogen. For example, the initial potential Hi = 543.5 mg HC/g $C_{org}$ corresponds to a mixture of 50% standard type-I kerogen with a relatively poor potential of 710 mg HC/g $C_{org}$ and 50% standard type-II kerogen with a poor potential of 377 mg HC/g $C_{org}$. The kinetic spectra of respective kerogen types were taken after Espitalie et al. [20].

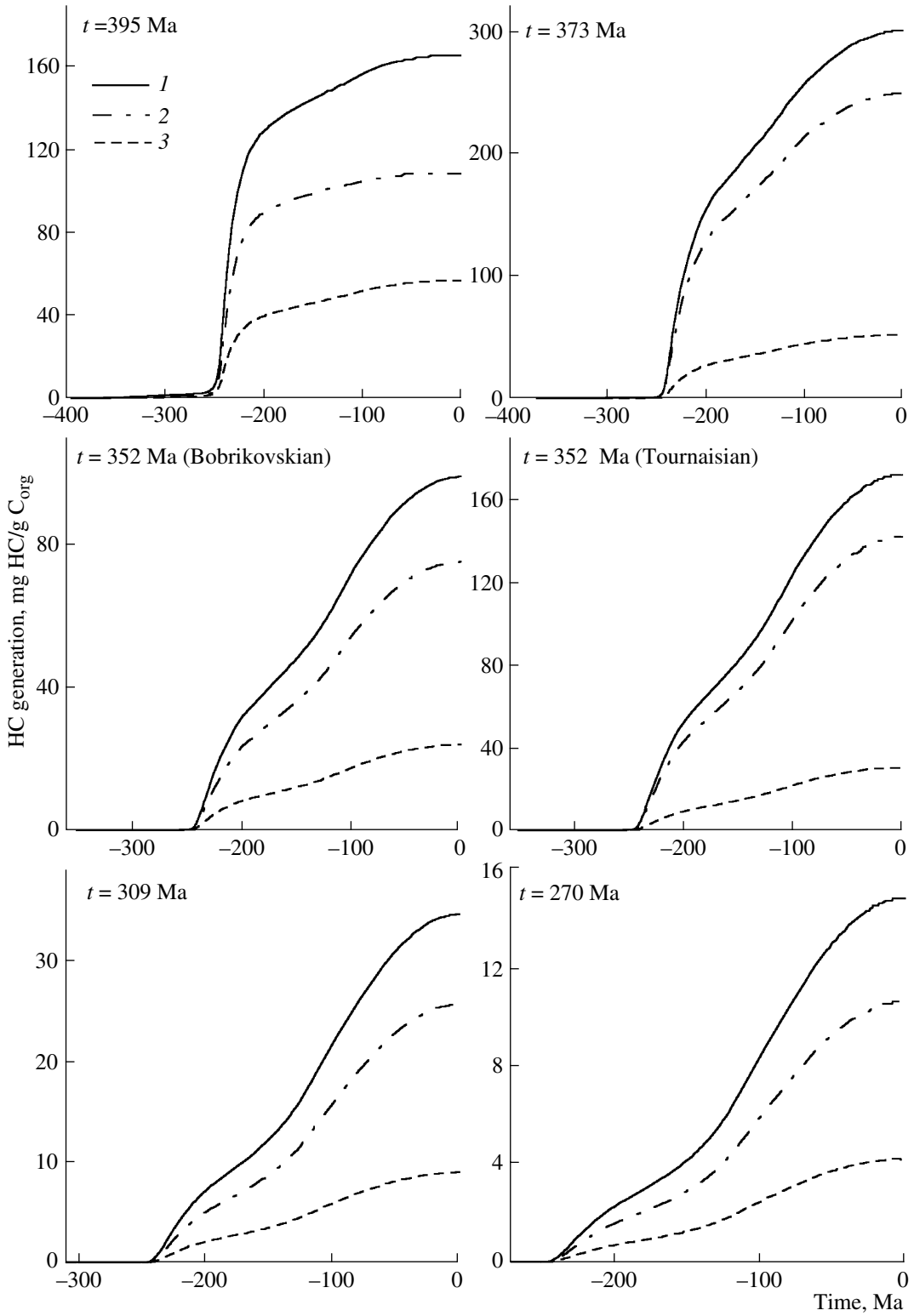


**Fig. 6.** Numerical reconstruction of the realization of the potential of HC generation in the subsidence history of the supposed source formations of the northern slope of the Precaspian Basin at the region of the Chinarevskaya prospect. The history of changes in the burial depth, temperature, and source rock maturity of the basin areas considered here is illustrated in Fig. 2. The supposed type and content of OM and the initial potential of HC generation are given in Table 5 for each of the supposed source formations. (*1*) Bulk yield of hydrocarbons (HC), (*2*) yield of liquid HC, and (*3*) yield of gaseous HC.

characterized by a considerable degree of the realization of the potential of HC generation coupled with relatively weak processes of secondary cracking in the deepest sequences of the Ural'skaya, Karachaganakskaya, and Yanvartsevskaya prospects (Table 3). According to Tables 3 and 5, the OM of the source rocks of the basin generates mainly liquid HC, although the fraction of gaseous HC becomes significant in the deeply buried levels of the Ural'skaya prospect. Note that the degrees of realization of the potential of HC generation shown in Table 3 are in agreement with the experimental pyrolysis of the source rocks. According to these data, the residual potential of HC generation by the Devonian rocks varies from 8 to 170 mg HC/g $C_{org}$ in the Karachaganskaya prospect and from 30 to 75 mg HC/g $C_{org}$ in the Chinarevskaya prospect [19]. The results of calculations presented in Table 3 are also consistent with the aforementioned data on the inflow of light sulfur-free oil from depths of 5647–5754 m and an oil–gas–water mixture from depths of 6120–6218 m in the Karachaganakskaya prospect [19].

The time of reaching the threshold of liquid HC emigration presented in Table 3 was estimated for a 20% filling of the pore space with liquid HCs [10, 18, 20]. The calculations took into account that the content of OM in the rocks could decrease appreciably in the course of its maturation and emigration. For instance, the initial $C_{org}$ content in the Late Devonian Frasnian sequences of the Ural'skaya prospect was estimated as 2.9% as compared with $C_{org}$ = 1.5% in the modern section. Note that the threshold of primary liquid HC emigration was not reached in the Middle Devonian rocks of the Chinarevskaya and Pavlovskaya prospects owing to insufficient generation of liquid HCs and low degree of rock compaction. The rocks of the same age from the Ural'skaya, Karachaganakskaya, Burlinskaya, and Yanvartsevskaya prospects reached this threshold (Fig. 2, Table 3). This process was aided by the high degree of liquid HC generation, the relatively high content of OM in the rocks, and the low porosity of deep-seated rocks. It is characteristic that the threshold of primary oil emigration from source rocks was always reached after the deposition of the salt complex, which served as a peculiar lid for the HC of the subsalt complex (Fig. 2).

## CONCLUSIONS

Our modeling showed that the difference between the sedimentary sections of the basin in the position relative to salt diapirs and thickness of salt horizons significantly affects the thermal history of OM maturation in the source rocks of the areas considered here. Our calculations were based on the present-day thicknesses of evaporite sequences and the suggestion that the time interval of their formation corresponded to the age of rock deposition (Kungurian and, in part, Kazanian stages). Therefore, the results of modeling can be corrected to account for the mechanism and time of formation of salt bodies. Unfortunately, this problem, including the dynamics of salt diapir growth, is not yet fully understood. For instance, there is still no adequate explanation for the absence of apparent deformations in the host rocks around salt diapirs. The geological database on the timing and rate of salt diapir formation and the trigger mechanism of its growth is very limited. At the present level of knowledge, we can only state that the generation properties of rocks are somewhat overestimated in our calculations for the regions between diapirs and underestimated for the rocks beneath salt diapirs. However, the degree of underestimation or overestimation strongly depends on the time and dynamics of salt diapir formation, and these characteristics are poorly constrained. The presented results allow us to estimate the possible variations in the conditions of petroleum generation for the rocks underlying the saline complex of the basin and in their temperature history related to the uncertainty of our knowledge on the time and rate of salt diapir formation. The results of our modeling can be considered as a reasonable approach to the description of the thermal history of the basin and generation properties of its source rocks, which will be refined as new information will be acquired from temperature measurements in boreholes, more sophisticated estimates of the degree of OM maturation in sedimentary rocks, and dynamic modeling of salt diapir formation.

## REFERENCES

1. R. G. Garetskii, L. G. Kiryukhin, I. N. Kapustin, and V. S. Konishchev, *Uncompensated Depressions of the East European Platform* (Nauka i Tekhnika, Minsk, 1990) [in Russian].
2. G. A. Cheremenskii, *Geothermy* (Nedra, Leningrad, 1972) [in Russian].
3. V. V. Kotrovskii, *Geothermal Conditions of the Formation and Localization of Hydrocarbon Reservoirs in the Sedimentary Cover of the Caspian Depression* (Saratov. Univ., Saratov, 1986) [in Russian].
4. M. J. Osborne and R. E. Swarbrick, "Mechanisms for Generating Overpressure in Sedimentary Basins: A Reevaluation," Am. Assoc. Petrol. Geol. Bull. **81**, 1023–1041 (1997).
5. E. V. Artyushkov, *Physical Tectonics* (Nauka, Moscow, 1993) [in Russian].
6. S. V. Aplonov, *Geodynamics of Deep Sedimentary Basins* (TsGI TETIS, St. Petersburg, 2000) [in Russian].
7. A. J. Baer, "Geotherms, Evolution of the Lithosphere and Plate Tectonics," Tectonophysics **72**, 203–227 (1981).
8. J. F. Schatz and G. Simmons, "Thermal Conductivity of Earth Materials at High Temperatures," J. Geophys. Res. **77**, 6966–6983 (1972).
9. Sh. Sh. Zaurbekov, Candidate's Dissertation in Geology and Mineralogy (Mosk. Gos. Univ., Moscow, 1988).
10. M. Makhous and Y. Galushkin, *Basin Analysis and Modeling of the Burial, Thermal and Maturation Histories in Sedimentary Basins* (Editions TECHNIP, Paris, 2005).

11. Yu. I. Galushkin, O. I. Simonenkova, and N. V. Lopatin, "Effect of the Giant Gas Pool Formation on the Thermal Regime of Sedimentary Sequence at the Urengoi Field in the West Siberian Basin," Geokhimiya, No. 12, 1335–1344 (1999) [Geochem. Int. **37**, 1203–1211 (1999)].

12. Yu. I. Galushkin and G. E. Yakovlev, "Thermal Evolution of the Lithosphere in the Bashkirian Sector of the West Ural Foothills as Compared with the Present-Day Thermal Regime of the Tagil–Magnitogorsk Zone of the Urals," Geotektonika, No. 6, 28–42 (2003) [Geotectonics **37**, 457–470 (2003)].

13. Ya. B. Smirnov, *Thermal Field of the USSR Territory: Explanatory Note to the 1 : 10000000 Map of Heat Flow and Deep Temperatures* (GUGK, Moscow, 1980) [in Russian].

14. Yu. I. Galushkin and R. I. Kutas, "Thermal Evolution of the Dnieper–Donets Paleorift and Applications to the Problems of Oil and Gas Potential," Geofiz. Zh. **17** (3), 13–23 (1995).

15. L. A. Frakes, *Climates throughout Geological Time* (Elsevier, Amsterdam, 1979).

16. *Changes in Climate and Landscapes over the Past 65 Ma (Cenozoic: from Paleocene to Holocene)*, Ed. by A. A. Velichko (GEOS, Moscow, 1999) [in Russian].

17. J. J. Sweeney and A. K. Burnham, "Evolution of a Simple Model of Vitrinite Reflectance Based on Chemical Kinetics," Am. Assoc. Petrol. Geol. Bull. **74**, 1559–1570 (1990).

18. Yu. I. Galushkin, G. E. Yakovlev, and V. F. Kuprin, "Catagenesis of Riphean and Vendian Deposits in Western Bashkortostan and Realization of the Hydrocarbon Potential of Their Organic Matter: Numerical Estimates," Geokhimiya, No. 1, 82–93 (2004) [Geochem. Int. **42**, 67–76 (2004)].

19. V. A. Konyukhova, Candidate's Dissertation in Geology and Mineralogy (Mosk. Gos. Univ., Moscow, 1999).

20. J. Espitalie, P. Ungerer, I. Irvin, and E. Marquis, "Primary Cracking of Kerogens. Experimenting and Modelling C1, C2-C5, C6-C15 Classes of Hydrocarbons Formed," Org. Geochem. **13**, 893–899 (1988).